

## Research Article

## Parametric Study of Reinforcement of Keyhole-less Friction Stir Spot Welding Using Al<sub>2</sub>O<sub>3</sub> and TiO<sub>2</sub> Nanopowders

M. Salehi<sup>1</sup>, S.M.H. Seyedkashi<sup>1\*</sup>, M. Sajed<sup>2</sup> and H. Rastegari<sup>3</sup>

<sup>1</sup> Mechanical Engineering Department, University of Birjand, Birjand 97175-376, Iran

<sup>2</sup> Mechanical Engineering Department, Azarbaijan Shahid Madani University, Tabriz, Iran

<sup>3</sup> Department of Mechanical and Materials Engineering, Birjand University of Technology, Birjand, Iran

## ARTICLE INFO

*Article history:*

Received 17 May 2023

Reviewed 17 July 2023

Revised 31 July 2023

Accepted 6 August 2023

*Keywords:*

Two-stage refilling friction stir spot welding  
Mild steel  
Nanopowder  
Joint strength

*Please cite this article as:*

M. Salehi, S.M.H. Seyedkashi, M. Sajed, H. Rastegari, Parametric Study of Reinforcement of Keyhole-less Friction Stir Spot Welding using Al<sub>2</sub>O<sub>3</sub> and TiO<sub>2</sub> Nanopowders, *Iranian Journal of Materials Forming*, 10(2) (2023) 55-67.

## ABSTRACT

In the present paper, two-stage refilled friction stir spot welding is used to join mild steel sheets with a thickness of 2 mm. Meanwhile, alumina and titanium oxide nanopowders are also introduced to the nugget to achieve superior mechanical properties. Two non-consumable tools are used with and without pins to weld and refill the keyhole, respectively. Before refilling, the keyhole is filled with nanopowders which are then distributed by the pinless refilling tool. Three parameters are investigated; the rotational speed of the welding tool, the rotational speed, and the dwell time of the refilling tool. The tensile test is used to evaluate the strength of the joints. The microhardness is measured in the welding zone to evaluate the powder distribution. The results suggest an increase in the joint strength by 42% and 18% with alumina and TiO<sub>2</sub> being used as a reinforcement, respectively. With a 31.94% contribution, the refilling tool rotational speed is the most effective input parameter affecting the joint strength. Considering the microstructure analysis and the microhardness test, the material flow pattern is mainly downward which results in the accumulation of the reinforcing powder in the lower sheet especially when a lower refilling tool rotational speed is used.

© Shiraz University, Shiraz, Iran, 2023

### 1. Introduction

Friction stir welding is a new solid-state welding procedure used to weld different materials including metals and polymers. This process is generally carried out on lightweight metals, mainly aluminum alloys, as well as different grades of steel [1]. A considerable fraction of alloys is used in the form of sheets, i.e., with

thicknesses in the range of 1 to 5 mm, making welding of sheets an important subject in industries and academic communities. Friction stir spot welding (FSSW) is a variant of the friction stir welding process that is used on sheet metals with a thickness of 2 mm or less [2]. The two main drawbacks of this process are the remaining keyhole and the limited strength of the joint. The conventional tool of friction stir spot welding contains a

\* Corresponding author

E-mail address: [seyedkashi@birjand.ac.ir](mailto:seyedkashi@birjand.ac.ir) (S.M.H. Seyedkashi)

<https://doi.org/10.22099/IJMF.2023.47414.1257>

cylindrical pin and a shoulder. During the welding, the pin penetrates the lower sheet where a hole is left behind when the tool is drawn out. This hole is known as the keyhole.

Several techniques are introduced to remove the keyhole and produce spot joints with no keyhole and better mechanical properties. Sajed [3] proposed the two-stage friction stir spot welding which is a cost-effective procedure to produce spot joints with no keyhole. Wu et al. [4] applied swing friction stir spot welding in the dissimilar welding of aluminum and magnesium alloy. In this process, the welding tool moves in a circular pattern. They reported an improvement in both the bonding area and material mixing. The same procedure was used by Guishen et al. [5] to join Al6061-T6 thin sheets. The refilling friction stir spot welding is a process in which the tool is made of parts that can move independently so that the spot joints can be produced in one step with no keyhole. Double-sided welding is a procedure to weld the joint on both sides where no keyhole is left. Wang et al. [6] used this procedure to weld low-carbon steels.

Many efforts have been made to reinforce the joints that were created by friction stir spot welding. In this regard, adding reinforced powders is a very common choice based on the knowledge that has been provided on friction stir processing of alloys [7]. Sadeghi et al. [8] investigated steel joints when TiO<sub>2</sub> was added. They investigated the effect of different contents of TiO<sub>2</sub> on the microstructure and mechanical properties of the joints. They reported a tool rotational speed of 1120 rpm and a dwell time of 9 s as the optimum input parameters. They also reported a 1.14 wt.% of the reinforcing powder as the optimum value to achieve the best mechanical properties. Sajed and Seyedkashi [9] developed a technique based on the two-stage friction stir spot welding to add SiC powder to spot joints of polyethylene sheets. They achieved a homogenized powder distribution and concluded that the refilling tool shoulder diameter is the most effective parameter. Alumina nanopowder was used by Enami et al. [10] to enhance the mechanical properties of Al2024 spot joints. Adibeig et al. [11] investigated a hybrid metal-polymer

joint in which an adhesive was used to reinforce the joint. They reported that the dwell time was the most effective parameter. They also achieved a remarkable increase in the strength of the joint by applying the adhesive due to a reduction in the stress gradient in the weld zone.

An interlayer is sometimes used to achieve better results. For instance, Gao et al. [12] used a Zn interlayer in the welding of copper and aluminum alloys and reported that the self-reacting behavior of the Zn resulted in obtaining sound welds. Wang et al. [13] discussed improving the mechanical properties of spot joints of AA2014 aluminum sheets when graphene nanosheets were used to strengthen the tip of the hook defect in the refilled friction stir spot welding. They reported an improvement in the tensile/shear strength and fracture toughness of the joint by 31% and 20%, respectively, when 0.6 wt.% of graphene nanosheets were applied.

The Welding of different grades of steel is an interesting research area. Although most steel alloys are considered to have good weldability, special considerations should be considered for some grades, such as high carbon ones. On the other hand, fusion welding has several problems in its nature including porosity, spattering, and hot cracking to name a few. Friction stir welding as a solid-state welding process yields high-strength joints with no melting defects. Because of that, many researchers studied friction stir welding and friction stir spot welding of steels. For example, Feng et al. [14] studied the feasibility of friction stir spot welding of high-strength steel alloys using a tool made of polycrystalline cubic boron nitride. Wang et al. [6] used a double-sided flat tool to join low-carbon steel sheets where the hook defect was also eliminated in addition to the keyhole. The same process was applied to ultra-high-strength C-Mn-Si martensitic steel [15]. Welding of dissimilar steel/aluminum joints is also an interesting field of investigation and the technology and characterization of these types of joints are discussed in the literature [16, 17].

The reinforcing of the spot joints was investigated by several authors; however, the present study is not the same. In many studies done previously, the plate is

reinforced before welding [18, 19]. Adding the reinforcing powder during welding is a challenging procedure and this is why in many cases, it is desired to add the reinforcing element before the joining process. In the present work, the reinforcing powder is added to the joint during the welding process. The nature of the process applied here, which is done in two steps, makes it possible to add the reinforcing powder during the welding. In the process that is reported by Enami et al. [10], again, the nanopowder is placed in a hole on the back of the upper sheet before welding. On the other hand, in their process, the sheets should also move in addition to changes that are made in the tool which makes the process even longer in time in comparison to the process that is presented here.

In the present study, a process based on the two-stage friction stir spot welding was applied to join low carbon steel sheets while alumina and  $TiO_2$  nanopowders were added to enhance the joint strength as well as the elimination of the keyhole. The main novelty of the present paper is the introduction of a cost-effective method capable of addressing both drawbacks of friction stir spot welding. The two drawbacks are the low strength of the joint, because the joint took place in just one point which is a common problem in spot joints using any welding method. The second drawback that is special for friction stir welding is the remaining keyholes after the welding due to the geometry of the welding tool. In the present paper, the keyhole is removed using a flat refilling tool in the second step. This also strengthens the joint by removing this defect and also increasing the load-carrying area. However, the main method of increasing the strength of the joint in this paper is to add the reinforcing powder after the welding and before refilling the joint; i.e. in the middle of the joining process. Thus, as mentioned above, both drawbacks of friction stir spot welding are addressed using the proposed method. The effects of welding parameters on mechanical properties were investigated and the performance of two nanopowders was compared. The process was able to significantly overcome both

issues in spot welding of mild steel sheets with a thickness of 1 mm.

## 2. Materials and Methods

In the present study, friction stir spot welding of mild steel sheets with a thickness of 1 mm, a length of 160 mm, a width of 40 mm, and an overlap length of 40 mm was investigated. The chemical composition of the welded sheet, which is presented in Table 1, is St12 or DIN 1.0330 alloy. Two-stage refilled friction stir spot welding (TFSSW), which was recently introduced by one of the authors [3], was applied to produce keyhole-less joints. In this process, two non-consumable tools are used in the welding and refilling stages. The schematic illustration of the process is presented in Fig. 1. The welding tool was a conventional friction stir welding tool with a conical pin the largest diameter of which is 3.5 mm and the smallest diameter is 3 mm with a length of 1.5 mm. The refilling tool is a flat shoulder pinless tool. The shoulders of both tools were 16 mm in diameter. Due to the high strength of steel, tungsten carbide is selected as the tool material. The tools' dimensions are presented in Fig. 2. Fig. 3 shows the fixture which was designed and fabricated to carry out the experiments.

**Table 1.** The chemical composition of the welded steel sheet (wt.%)

C	Si	Mn	P	S	Fe
0.037	0.032	0.236	0.005	0.005	Base

Since the process is carried out in two stages, the keyhole could be filled using a reinforcing powder

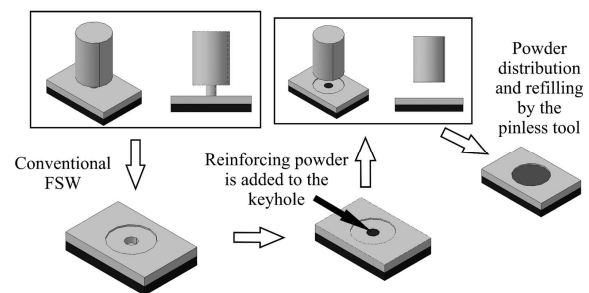


**Fig. 1.** The schematic illustration of the refilling two-stage friction stir spot welding; The first stage is the conventional FSSW. Then, the keyhole is filled with the reinforcing powder. The distribution of the powder took place by a pinless tool.

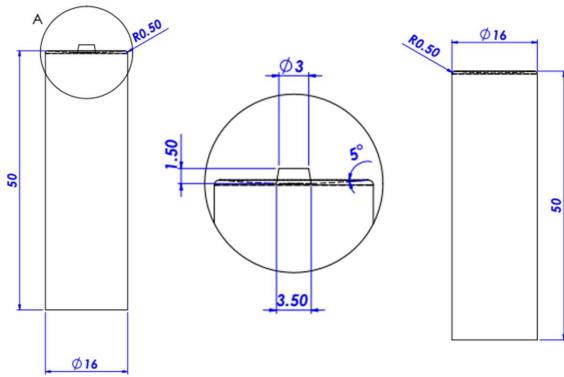


Fig. 2. Welding and refilling tools. The dimensions of the pin are presented in the detail view. The pinless refilling tool is also presented.

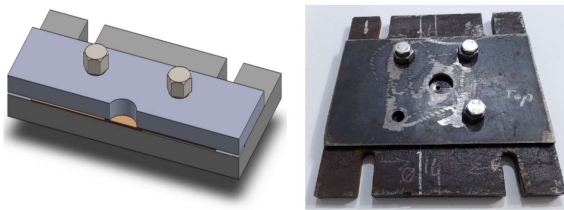


Fig. 3. The welding fixture and its section view; The fixture is needed to clamp the joining sheets and avoid their deformation during welding.

before the refilling stage. In the present study, alumina and  $\text{TiO}_2$  nanopowders were introduced to the nugget and the effects of welding parameters on powder distribution and enhancement in mechanical properties were investigated. The keyhole space was filled with reinforcing powders before the refilling stage. Thus, the volume of reinforcing powder is the same for all experiments. Effects of the addition of nanopowders on the mechanical properties of the joints were also compared. The SEM images of nanopowders and corresponding EDS analyses are presented in Fig. 4. The details of these powders are as follows:

- 1)  $\text{Al}_2\text{O}_3$ , alpha, +99%, 50 nm, US Research Nanomaterials Inc.
- 2)  $\text{TiO}_2$ , rutile, +99.9%, 30 nm, US Research Nanomaterials Inc.

The welding tool rotational speed, refilling tool rotational speed, and refilling tool dwell time are the investigated parameters. These parameters and their corresponding levels are summarized in Table 2. The tool

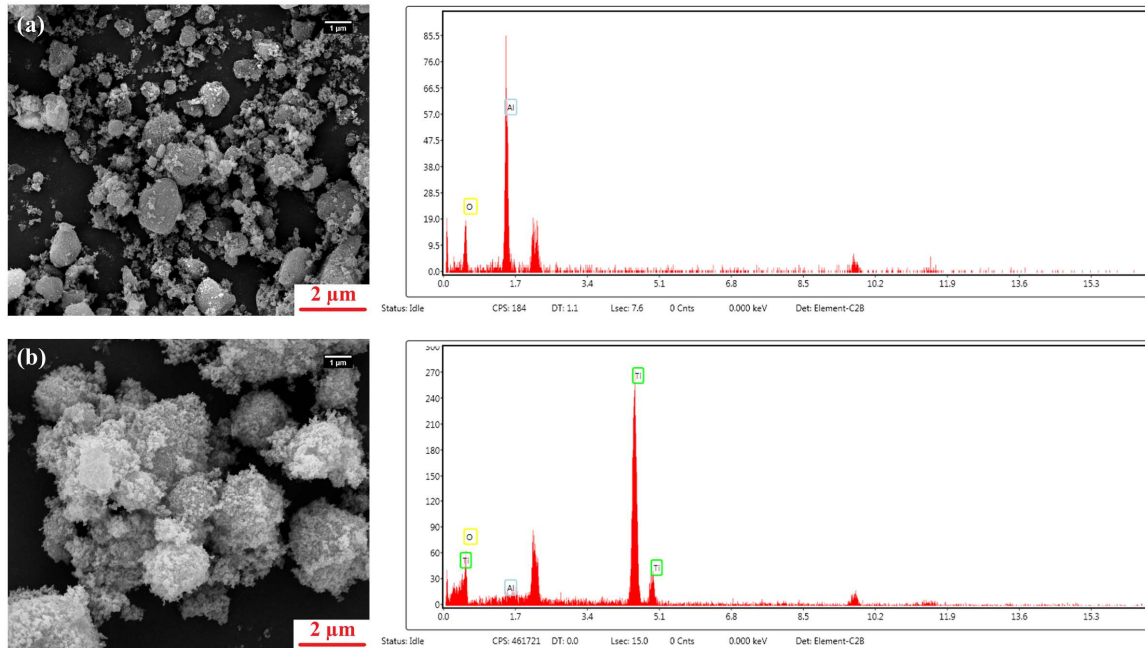


Fig. 4. The SEM images of reinforcing powders and the related EDS analysis: (a)  $\text{Al}_2\text{O}_3$ , and (b)  $\text{TiO}_2$ .

Table 2. The levels of investigated parameters

Parameter	Unit	Level 1	Level 2	Level 3
Welding tool rotational speed	rpm	1000	1600	2500
Refilling tool rotational speed	rpm	1000	1600	2500
Refilling tool dwell time	s	4	6	8

rotational speed is the main parameter in friction stir spot welding and its best range is between 1000 to 2500 rpm [20]. This range is also used in the present paper. All parameters are investigated in three levels. Thus, considering a full factorial design of experiments, 27 sets of treatments were investigated which are summarized in Table 3. These 27 tests were carried out using alumina nanopowder as the reinforcing powder. To compare the strength of the joint when TiO<sub>2</sub> nanopowder is introduced and also when no powder is added to the nugget, six extra sets of tests were also performed using the optimum conditions, i.e., the treatments that obtained the highest strength. The tensile test was used to evaluate joint strength. A tensile test machine with a Zwick controller was used to carry out the tests using a speed of 1 mm/min. The results of tensile strength are summarized in Table 3. Optical microscopy, using a Dewinter optical microscope, was used to evaluate the

microstructure and the powder distribution. The standard procedure was used to mount the samples and the 2% Nital etchant was used to etch them. M5 Vickers hardness test machine was used to carry out the microhardness test with a force of 100 g and a period of 10 s according to the presented strategy in Fig. 5. Due to symmetry, microhardness values were just measured on one side of the weld cross-section. To investigate the powder distribution in both sheets, both upper and lower sheets were considered in the microhardness measurement strategy. The measurement points were distributed on the joint cross-section in such a way to cover all the microstructural zones including stir zone (SZ), thermo-mechanically affected zone (TMAZ), heat affected zone (HAZ), and base metal (BM). FEI ESEM QUANTA scanning electron microscope equipped with EDS analysis was used to investigate the distribution of the nanopowders and the fracture surface of the joints.

**Table 3.** The experiments and corresponding joint strength and extension using alumina nanopowder

No.	Welding tool rotational speed (rpm)	Refilling tool rotational speed (rpm)	Refilling tool dwell time (s)	Joint strength (N)	Joint extension (mm)
1	1600	2500	8	10313	12.99
2	1000	1600	4	7934	5.93
3	1600	1600	6	9203	6.55
4	1600	1000	8	7940	6.20
5	2500	1000	4	7774	2.18
6	1600	2500	6	10184	9.42
7	1600	1600	8	9571	11.18
8	1600	1000	4	8075	3.84
9	2500	1600	8	8388	2.72
10	1000	1600	6	7603	2.49
11	2500	1000	6	7793	2.82
12	1600	2500	4	10552	16.07
13	2500	2500	6	8995	3.61
14	2500	2500	4	8547	4.32
15	1000	2500	4	10288	11.22
16	2500	1600	6	8271	2.29
17	2500	1000	8	7824	3.61
18	1000	1000	8	7971	4.97
19	1000	2500	8	9908	3.76
20	1600	1600	4	9019	3.48
21	1600	1000	6	8063	3.44
22	2500	2500	8	9215	5.51
23	1000	1000	6	6849	2.02
24	1000	1600	8	7793	9.22
25	1000	2500	6	9865	14.03
26	1000	1000	4	6683	4.18
27	2500	1600	4	9191	7.41

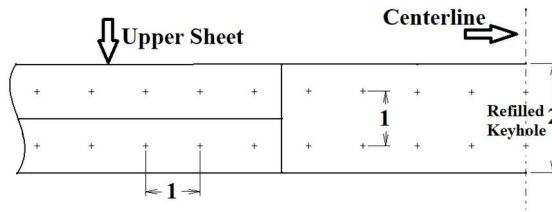


**Fig. 5.** The microhardness test strategy. Half of a typical cross-section of a welded sample is presented. The points represent hardness measurement sites.

### 3. Results and Discussion

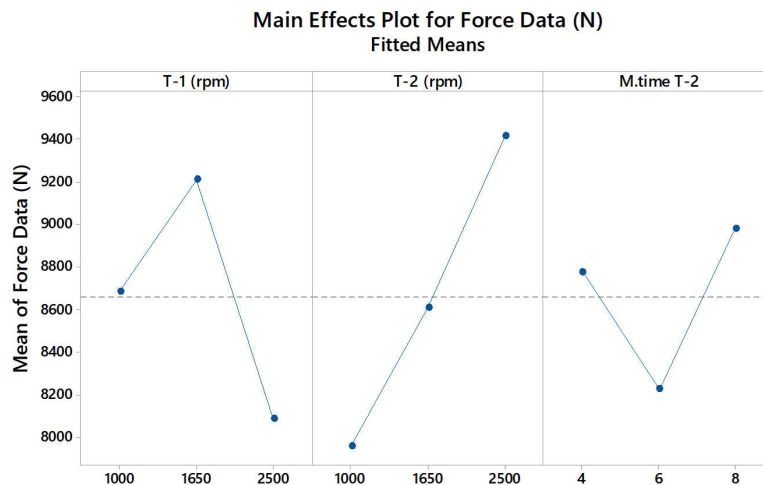
In the present study, a new variant of friction stir spot welding, namely two-stage refilled friction stir spot welding (TFSSW) is used to join mild steel sheets. Meanwhile, the reinforcement of the joint was also considered using  $\text{TiO}_2$  and  $\text{Al}_2\text{O}_3$  nanopowders. The process is a two-stage process, and the keyhole is filled with a reinforcing powder before the refilling stage.

#### 3.1. Effects of welding parameters on the joint strength

The joint strength of the first set of experiments, i.e. 27 experiments using the alumina nanopowder, were presented in Table 3. The analysis of variance (ANOVA) was employed to evaluate the effect of each processing parameter on the joint strength which is summarized in Table 4. The refilling tool rotational speed is the most effective parameter on the joint strength with a 31.94% contribution percentage while the welding tool rotational speed and refilling tool dwell time have contributed 19.02% and 9.14%, respectively. The results also indicate that the two-way interactions are not significant. The main effects plot is presented in Fig. 6. Any increase in the refilling tool rotational speed results in an increase in the strength of the joint where the maximum strength was obtained with the highest rotational speed (2500 rpm).

**Table 4.** ANOVA results of the effects of input parameters on joint strength

Source	DF	Seq SS	Contribution	F-Value	P-Value
Model	18	22643181	75.47%	1.37	0.337
Linear	6	18032402	60.10%	3.27	0.063
T-1 (rpm)	2	5708016	19.02%	3.10	0.101
T-2 (rpm)	2	9582266	31.94%	5.21	0.036
M.time T-2	2	2742120	9.14%	1.49	0.282
2-Way Interactions	12	4610779	15.37%	0.42	0.916
T-1 (rpm)×T-2 (rpm)	4	1339862	4.47%	0.36	0.828
T-1 (rpm)×M.time T-2	4	1606798	5.36%	0.44	0.779
T-2 (rpm)×M.time T-2	4	1664119	5.55%	0.45	0.769
Error	8	7360700	24.53%		
Total	26	30003881	100.00%		



All displayed terms are in the model.

**Fig. 6.** Main effects plot; The variation of the joint strength is presented versus conventional tool rotational speed (T-1), refilling tool rotational speed (T-2), and refilling tool dwell time (M.time T-2).

There is no traverse movement during the FSSW process, which makes it difficult to add any reinforcing powder to the nugget. When a nanopowder is going to be used, the agglomeration of the powder is also a serious problem which was indicated in the literature [10]. Several researchers preferred to use the reinforcement in the form of interlayer instead of powder [21]. The reinforcing powder agglomeration is also reported in similar friction-based processes [22]. Higher refilling tool rotational speed accelerates the powder distribution and results in a more homogenous distribution of the reinforcing powder. It seems to be the main reason for this type of correspondence between the refilling tool rotational speed and the joint strength. Fig. 7 presents a typical cross-section of a refilled specimen that was welded with a refilling tool rotational speed of 2500 rpm (sample No. 15). The joint strength (the maximum tensile-shear load that the joint can bear before failure) for this specimen is 10288 N. For this specimen, a homogenous distribution of alumina powder is evident. The dark zone in the image presents the stir zone, i.e. the zone where the reinforcing powder is distributed by the refilling pinless tool. There is no sign of agglomeration or lack of powder distribution in a part of the stir zone. On the other hand, higher heat input is required in the welding of the steel in comparison with aluminum or other lightweight metals [23]. The main source of the heat input is the tool rotational speed. Especially, when the spot joint is to be created. Higher tool rotational speed provides much more heat for the nugget which results in better stirring, bonding, and

higher joint strength. It also improves the viscoplastic behavior of the steel which results in a better material flow and stronger joints.

The increase of tool rotational speed at first increases and then decreases the joint strength; see Fig. 6. The increase of welding tool rotational speed from 1000 rpm to 1600 rpm increases the strength of the joints which is due to insufficient heating of the material when the tool rotational speed is 1000 rpm. However, when the welding tool rotational speed increases from 1600 rpm to 2500 rpm, the strength drops which may be the result of the coarsening of the microstructure due to the higher heat input. According to Table 3, the joint strengths of No. 3 which was welded with a welding tool rotational speed of 1600 rpm and refilling tool rotational speed of 1600 rpm, and specimen No. 9 which was welded with a welding tool rotational speed of 2500 rpm and refilling tool rotational speed of 1600 rpm are 9203 N and 8388 N, respectively. This indicates that an almost 1000 N higher strength was obtained when the lower tool rotational speed was applied. The HAZ region has the lowest microhardness in the welding zone. Considering the HAZ as a region where the crack initiates and propagates until failure [24], the investigation of microstructure in this zone could give an insight into this phenomenon. Figs. 8(a) and 8(b) present the HAZ in specimens No. 3 and No. 9, respectively. The coarsening of grains, as a result of higher heat input, is evident for specimen No. 9 that was welded with a higher welding tool rotational speed. The average grain size for specimen No. 3 is 115.4  $\mu\text{m}$  while it is 127.7  $\mu\text{m}$  for specimen No. 9. As mentioned above, the investigation of the HAZ zone is very important from a fracture studies point of view. However, there are other regions in the welding nugget with a different microstructure namely stir zone (SZ), thermo-mechanically affected zone (TMAZ), and base metal (BM). These zones together with the cross-section of sample No. 9 are presented in Fig. 9 as a typical microstructure for welded samples.

As a sheet that is subjected to friction stir spot welding procedure, different zones are formed in the microstructure of the joint which are presented in Fig. 9

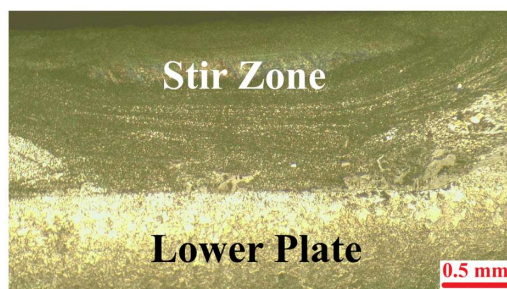


**Fig. 7.** A typical cross-section of the refilled specimen (sample No. 15 welded with a refilling tool rotational speed of 2500 rpm). The stir zone is marked in the picture (the dark zone).

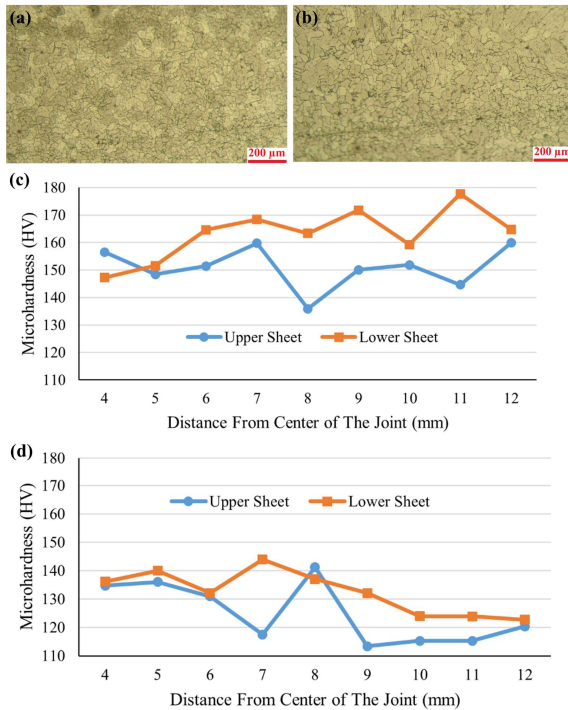


**Fig. 8.** Effect of welding tool rotational speed on grain growth: (a) HAZ in sample No. 3 with welding and refilling tool rotational speeds of 1600 rpm, (b) HAZ in sample No. 9 with welding and refilling tool rotational speeds of 2500 and 1600 rpm, respectively, (c) microhardness of welding zone in specimen No. 3, and (d) microhardness of welding zone in specimen No. 9.

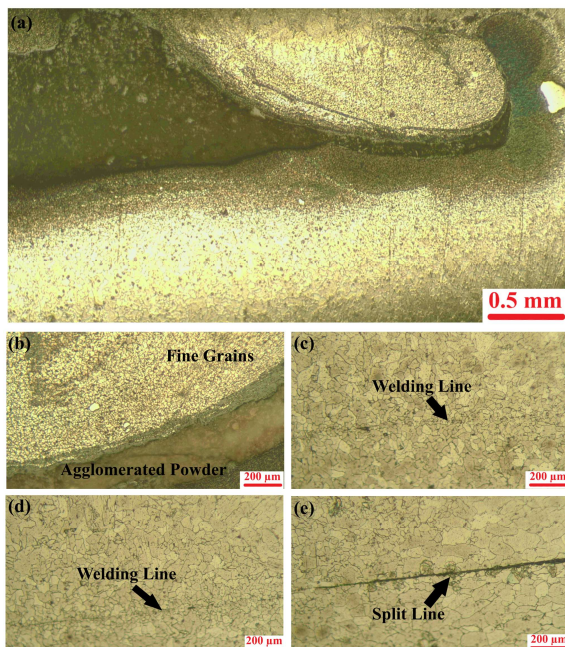


**Fig. 9.** Different zones in the weld cross-section of sample No. 9: (a) the weld cross-section, (b) the stir zone (SZ), (c) the thermomechanically affected zone (TMAZ), (d) the heat affected zone (HAZ), and (e) base metal (BS).

in detail. In Fig. 9(a), the cross-section of specimen No. 9 is presented where although the powder is distributed in the stir zone, the inhomogeneity in the powder distribution is evident. In Fig. 9(b), the stir zone is presented with more details. In this figure, two phenomena are marked, namely fine grains and powder agglomeration. The fine grains are presented due to the dynamic recrystallization during the welding which results in new equiaxed fine grains. For this specimen, the combination of input parameters, i.e. a welding tool rotational speed of 2500 rpm, a refilling tool rotational speed of 1600 rpm, and a refilling dwell time of 8 s, did not result in a homogenous distribution of reinforcing powder which is confirmed by the presence of agglomerated powder in the stir zone. The thermomechanically affected zone is a zone where the grains experience both mechanical work and heat; however, the microstructure is coarser in comparison with the stir zone which is presented in Fig. 9(c). In any welding procedure, there is a zone called heat affected zone, where grain growth takes place due to the heat generation during the welding. This zone is at a distance from the welding zone and should be limited to have a joint with a good strength. This zone is presented in Fig. 9(d). Fig. 9(e) presents the base metal and the split line which is far from the welding zone with no thermal or mechanical cycle experienced.

According to the results of the microhardness test, presented in Figs. 8(c) and 8(d) for specimens No. 3 and 9, respectively, the higher microhardness of specimen No. 3 as a result of finer grains is obvious. This could be considered as a reason for the higher strength of this specimen in comparison with specimen No. 9. Since the microhardness of the stir zone is much higher than other zones due to the presence of the reinforcing powder (more than 300 HV), these data were omitted from the graph to present the data on a more desirable scale. In both samples, the hardness of the lower sheet is higher than the upper one, although the difference is not significant. It indicates that more reinforcing particles are trapped in the lower one. The same difference was also obtained for other specimens. The main heat source in this process is the friction between the tool shoulder

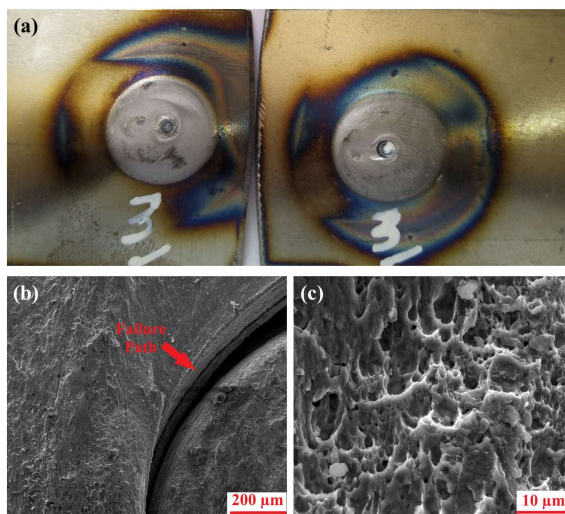
and the surface of the upper sheet. Thus, the upper sheet experiences more heat input and hence higher temperatures. The higher temperature provides a suitable environment for grain growth and a drop in microhardness. Fig. 10 presents the SEM images of specimen No. 3 after failure where the crack propagation path is marked in the figure.

The dependence of the joint strength on the refilling tool dwell time is different. An increase of the refilling tool dwell time at first decreases and then increases the joint strength when it changes from 6 s to 8 s. As mentioned before, the effect of refilling tool dwell time on the joint strength is negligible according to the ANOVA (9.14% contribution). For example, there is just less than a 4% difference (368 N) between the strengths of specimen No. 12 which is welded with a welding tool rotational speed of 1600 rpm, refilling tool rotational speed of 2500 rpm, and refilling tool dwell time of 4 s and specimen No. 6 which was welded with the same parameters but a refilling tool dwell time of 6 s. Increasing the refilling tool dwell time has two effects: (a) more heat input and subsequent grain coarsening, and (b) more stirring of the nanopowder and more homogenous distribution as a result. When the refilling tool dwell time increases from 4 s to 6 s, the first effect, i.e. grain coarsening, plays the main role and is responsible

for the decrease in the strength of the joint. But in the case of increasing the refilling dwell time from 6 s to 8 s, the second effect, i.e. higher homogeneity, is in charge and the strength even passes that of the first level.

### 3.2. Effect of reinforcing powder on the joint strength

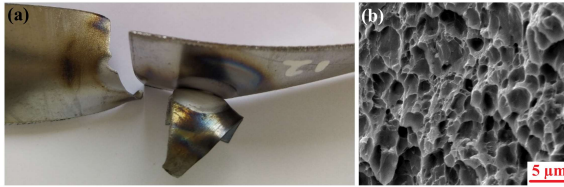
Table 5 presents the joint strengths for six experiments with the highest joint strength in three different conditions including no reinforcement, reinforcing with TiO<sub>2</sub>, and reinforcing with Al<sub>2</sub>O<sub>3</sub> which are called cases I, II, and III, respectively. The average joint strength in case I is 7170 N while it is 8487 N and 10185 N in cases II and III, respectively. This indicates an increase in the joint strength by 18% and 42% on average when TiO<sub>2</sub> and Al<sub>2</sub>O<sub>3</sub> are applied as the reinforcing powder, respectively. The highest joint strength is 10552 N which was obtained in case III and sample No. 12 that was welded by a welding tool rotational speed of 1600 rpm, refilling tool rotational speed of 2500 rpm, and dwell time of 4 s. Fig. 11 and Fig. 12 present the fracture mode and SEM images of the specimens that were welded by input parameters of the specimen No. 12 with reinforcing nanopowders of Al<sub>2</sub>O<sub>3</sub> and TiO<sub>2</sub>, respectively. Both specimens failed in ductile mode due to the presence of dimples; however, fracture happened in the base metal of the specimen reinforced with alumina while shear fracture took place for the specimen reinforced with TiO<sub>2</sub>. Case III presents a significantly higher joint strength which determines that Al<sub>2</sub>O<sub>3</sub> is a good choice to be used as the reinforcing powder when mild steel sheets are going to be welded using the friction stir spot welding process. Considering Table 3 the highest joint extension was also obtained for specimen No. 12 which is 16.07 mm while the average



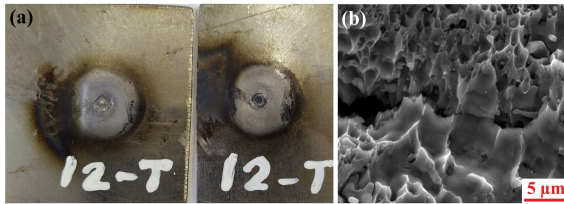
**Fig. 10.** Fractographic analysis of specimen No. 3: (a) the macrograph of failed specimen both lower and upper sheet, (b) the failure path of the joint, and (c) dimples in the failure surface indicating that a ductile fracture was happened.

**Table 5.** The experiments with the highest joint strength

No.	Case I: Primary joint strength (N)	Case II: Joint strength with TiO <sub>2</sub> (N)	Case III: Joint strength with Al <sub>2</sub> O <sub>3</sub> (N)
1	7394	8786	10313
6	7364	8553	10184
12	7394	8706	10552
15	6855	8007	10288
19	6849	8394	9908
25	7167	8473	9865



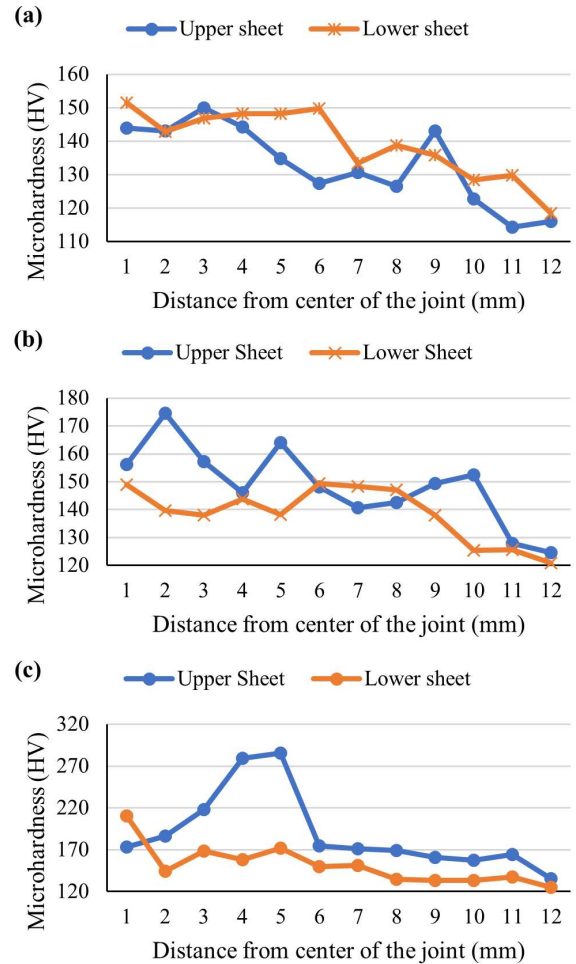
**Fig. 11.** (a) Fracture mode and (b) dimples on the fracture surface of specimen No. 12 reinforced with  $\text{Al}_2\text{O}_3$ . The fracture zone is placed in the base metal which indicates that a good joint is achieved.



**Fig. 12.** (a) Fracture mode and (b) dimples on the fracture surface of specimen No. 12 reinforced with  $\text{TiO}_2$ . Shear fracture mode occurs for the specimen in the welding zone.

value is 6.13 mm. In other words, the joint extension is increased by 162% for specimen No. 12 in comparison with the average value. This means that the highest joint strength and ductility could be achieved simultaneously when the alumina nanopowder is used to reinforce the joint if proper input parameters are considered.

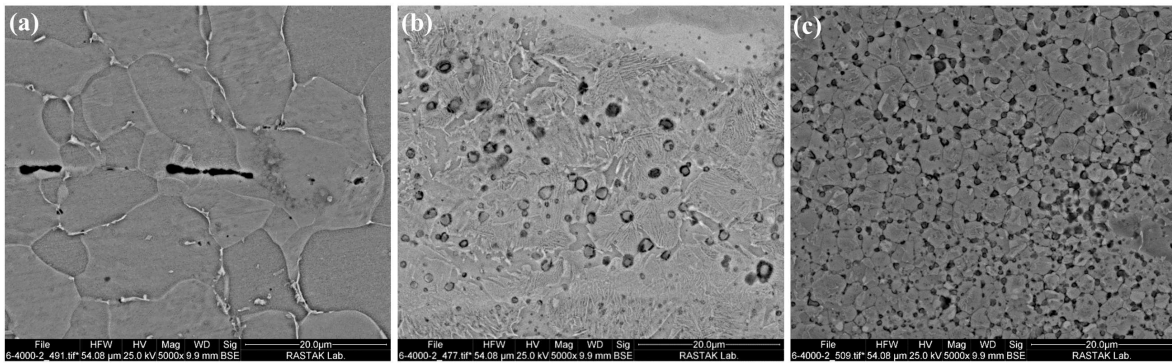
Fig. 13 presents the microhardness distribution for sample No. 12 in all three cases. In all cases, there is a decrease in the microhardness when the distance from the joint centerline is increasing. This is mainly due to the presence of the reinforcing powder in the joint stir zone. However, in case I, where no reinforcing powder is used, the same trend is detectable. In this case, the microhardness is higher in the stir zone due to severe plastic deformation and dynamic recrystallization that occurs during the welding process. The coarsening in the microstructure when the distance increases from the center of the joint is evident in the image which is the reason for the drop in the microhardness together with the presence of the reinforcing powder. The maximum hardness for cases I, II, and III are 151.44, 174.47, and 285.45 HV, respectively, where again a significantly higher microhardness is observed for case III. The material flow direction is mainly downward in both stages which results in more powder accumulation in the lower sheet and a higher microhardness as a result.



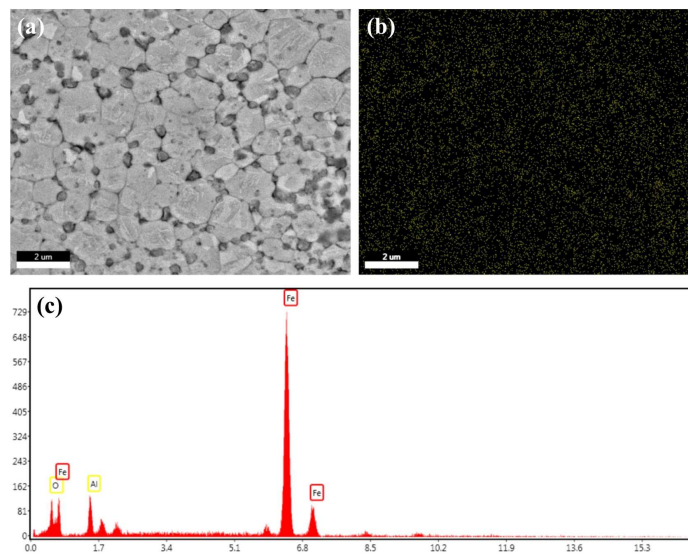
**Fig. 13.** Microhardness profile of samples welded by the parameters of specimen No. 12, i.e. a welding tool rotational speed of 1600 rpm, a refilling tool rotational speed of 2500 rpm, and a refilling tool dwell time of 4s: (a) Case I welded with no reinforcing powder, (b) Case II welded by adding  $\text{TiO}_2$  powder, and (c) Case III welded by adding  $\text{Al}_2\text{O}_3$  powder.

Fig. 14 presents the microstructure of the stir zone in different specimens welded by the parameters of specimen No. 12. For cases II and III the presence of reinforcing powder is evident. In Case III, the grains are very fine compared to Case I where no powder is used. Because the welding parameters were the same for all three specimens, the reason for this difference is the presence of  $\text{Al}_2\text{O}_3$  powder and the pinning effect which is reported in the literature too [25]. This phenomenon happened for Case II too; however, the effect is stronger when  $\text{Al}_2\text{O}_3$  is used.

Fig. 15 and Fig. 16 present the EDS analysis for the specimen reinforced with  $\text{Al}_2\text{O}_3$  and  $\text{TiO}_2$ , and also the



**Fig. 14.** Microstructure of stir zone in different specimens welded by the parameters of specimen No. 12, i.e. a welding tool rotational speed of 1600 rpm, a refilling tool rotational speed of 2500 rpm, and a refilling tool dwell time of 4 s: (a) Case I welded with no reinforcing powder, (b) Case II welded by adding  $TiO_2$  powder, and (c) Case III welded by adding  $Al_2O_3$  powder.



**Fig. 15.**  $Al_2O_3$  reinforced specimen: (a) SEM microstructure, (b) Al map, (c) EDS analysis.

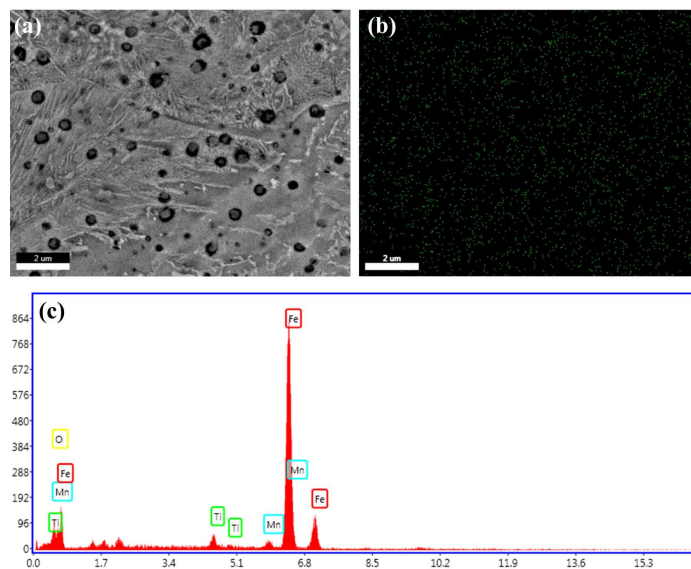


**Fig. 16.**  $TiO_2$  reinforced specimen: (a) SEM microstructure, (b) Ti map, (c) EDS analysis.

corresponding Al and Ti maps. These specimens were welded by the parameter set of experiment No. 12. The homogenous distribution of the reinforcing powder which is evident in these figures is considered to be the main reason for the highest strength obtained with this experimental set. According to the EDS analysis that is provided in Fig. 15(c) and Fig. 16(c), the presence of reinforced particles, i.e.  $\text{Al}_2\text{O}_3$  and  $\text{TiO}_2$ , is confirmed.

#### 4. Conclusion

In the present study, mild steel sheets with a thickness of 1 mm were welded using the two-stage friction stir spot welding process.  $\text{Al}_2\text{O}_3$  and  $\text{TiO}_2$  nanopowders were used as reinforcing powders. The effects of welding parameters including the welding tool rotational speed, refilling tool rotational speed, and refilling tool dwell time were investigated on joint strength, microstructure, and microhardness. Two reinforcing powders were also compared. The fracture analysis was also carried out to gain a better insight into the process. The main results are as follows:

- The hardness and strength together with the extension of joints are higher when nanopowders are used. The mechanical characteristics are significantly improved when  $\text{Al}_2\text{O}_3$  nanopowder is used as reinforcement.
- The contribution order of the input parameters concerning the strength of the joints are as follows: the refilling tool rotational speed, refilling tool dwell time, and welding tool rotational speed.
- Any increase in the refilling tool rotational speed results in higher strength due to two reasons: more homogenous distribution of the reinforcing powder and more heat input which improves the viscoplastic behavior of the steel.
- The main fraction of the reinforcing powder remains in the lower sheet due to the material flow pattern during the welding. The powder is even trapped in the lower sheet when a lower refilling tool rotational speed is used.

#### Conflict of Interests

The Authors declare that there is no conflict of interest.

#### Funding

The authors received no financial support for the research, authorship, and/or publication of this article.

#### 5. References

- [1] S. Sattari, H. Bisadi, M. Sajed, Mechanical properties and temperature distributions of thin friction stir welded sheets of AA5083, *International Journal of Mechanics and Applications*, 2(1) (2012) 1-6.
- [2] J. Derogar, S.M.H. Seyedkashi, M. Sajed, Experimental study of friction stir spot welding of a non-alloyed aluminium sheet with stationary shoulder, *Karafan Quarterly Scientific Journal*, 19(3) (2022) 141-161.
- [3] M. Sajed, Parametric study of two-stage refilled friction stir spot welding, *Journal of Manufacturing Processes*, 24 (2016) 307-317.
- [4] S. Wu, T. Sun, Y. Shen, Y. Yan, R. Ni, W. Liu, Conventional and swing friction stir spot welding of aluminum alloy to magnesium alloy, *The International Journal of Advanced Manufacturing Technology*, 116(7) (2021) 2401-2412.
- [5] Y. Guishen, C. Xin, W. Zitao, Mechanical performance optimization and microstructure analysis of similar thin AA6061-T6 sheets produced by swept friction stir spot welding, *The International Journal of Advanced Manufacturing Technology*, (2021) 1-13.
- [6] X. Wang, Y. Morisada, H. Fujii, Flat friction stir spot welding of low carbon steel by double side adjustable tools, *Journal of Materials Science & Technology*, 66 (2021) 1-9.
- [7] J. Iwaszko, M. Sajed, Technological aspects of producing surface composites by friction stir processing —A review, *Journal of Composites Science*, 5(12) (2021) 323.
- [8] B. Sadeghi, H. Abbasi, M. Atapour, S. Shafiee, P. Cavaliere, Z. Marfavi, Friction stir spot welding of  $\text{TiO}_2$  nanoparticle-reinforced interstitial free steel, *Journal of Materials Science*, 55 (2020) 12458-12475.
- [9] M. Sajed, S.M.H. Seyedkashi, A novel technique for keyhole-less reinforced friction stir spot welding of polyethylene sheets, *ADMT Journal*, 12(4) (2019) 47-56.
- [10] M. Enami, M. Farahani, M. Farhang, Novel study on keyhole less friction stir spot welding of Al 2024

- reinforced with alumina nanopowder, *The International Journal of Advanced Manufacturing Technology*, 101(9) (2019) 3093-3106.
- [11] M.R. Adibeig, G. Marami, M.A. Saeimi-Sadigh, L.F.M. da Silva, Experimental and numerical study of polyethylene hybrid joints: friction stir spot welded joints reinforced with adhesive, *International Journal of Adhesion and Adhesives*, 98 (2020) 102555.
- [12] P. Gao, Y. Zhang, K.P. Mehta, Metallurgical and mechanical properties of Al-Cu joint by friction stir spot welding and modified friction stir clinching, *Metals and Materials International*, 27(8) (2021) 3085-3094.
- [13] S. Wang, X. Wei, J. Xu, J. Hong, X. Song, C. Yu, J. Chen, X. Chen, H. Lu, Strengthening and toughening mechanisms in refilled friction stir spot welding of AA2014 aluminum alloy reinforced by graphene nanosheets, *Materials & Design*, 186 (2020) 108212.
- [14] Z. Feng, M.L. Santella, S.A. David, R.J. Steel, S.M. Packer, T. Pan, M. Kuo, R.S. Bhatnagar, Friction stir spot welding of advanced high-strength steels—a feasibility study, *SAE Transactions*, (2005) 592-598.
- [15] X. Wang, Y. Morisada, K. Ushioda, H. Fujii, Double-sided friction stir spot welding of ultra-high strength C-Mn-Si martensitic steel by adjustable probes, *Journal of Materials Processing Technology*, 300 (2022) 117422.
- [16] K. Kumamoto, T. Kosaka, T. Kobayashi, I. Shohji, Y. Kamakoshi, Microstructure and fatigue behaviors of dissimilar A6061/galvannealed steel joints fabricated by friction stir spot welding, *Materials*, 14(14) (2021) 3877.
- [17] T. Matsuda, T. Ogaki, K. Hayashi, C. Iwamoto, T. Nozawa, M. Ohata, A. Hirose, Fracture dominant in friction stir spot welded joint between 6061 aluminum alloy and galvannealed steel based on microscale tensile testing, *Materials & Design*, 213 (2021) 110344.
- [18] H. Dong, Z. Tang, P. Li, B. Wu, X. Hao, C. Ma, Friction stir spot welding of 5052 aluminum alloy to carbon fiber reinforced polyether ether ketone composites, *Materials & Design*, 201 (2021) 109495.
- [19] Y. Ogawa, H. Akebono, K. Tanaka, A. Sugeta, Effect of welding time on fatigue properties of friction stir spot welds of Al to carbon fibre-reinforced plastic, *Science and Technology of Welding and Joining*, 24(3) (2019) 235-242.
- [20] Z. Shen, Y. Ding, A.P. Gerlich, Advances in friction stir spot welding, *Critical Reviews in Solid State and Materials Sciences*, 45(6) (2020) 457-534.
- [21] O. Kalaf, T. Nasir, M. Asmael, B. Safaei, Q. Zeeshan, A. Motalebzadeh, G. Hussain, Friction stir spot welding of AA5052 with additional carbon fiber-reinforced polymer composite interlayer, *Nanotechnology Reviews*, 10(1) (2021) 201-209.
- [22] M. Sajed, S.M.H. Seyedkashi, Solid-state local micro-alloying of thick st37 steel plates with SiC powder using a modified friction hydro-pillar process, *Journal of Materials Research and Technology*, 9(4) (2020) 7158-7171.
- [23] S. Memon, J. Tomków, H.A. Derazkola, Thermo-mechanical simulation of underwater friction stir welding of low carbon steel, *Materials*, 14(17) (2021) 4953.
- [24] M. Sajed, H. Bisadi, Experimental failure study of friction stir spot welded similar and dissimilar aluminum alloys, *Welding in the World*, 60 (2016) 33-40.
- [25] M. Farshbaf Ahmadipour, M. Movahedi, A.H. Kokabi, Microstructural evaluation and mechanical properties of Al1050/TiO<sub>2</sub>-graphite hybrid nanocomposite produced via friction stir processing, *Metallurgical and Materials Transactions A*, 50 (2019) 2443-2461.